Article

One-dimensional lead-free halide with near-unity greenish-yellow light emission

Sai Li, Jun Xu, Zhigang Li, Zhichao Zeng, Wei Li, Minghuan Cui, ChaoChao Qin, and Yaping Du

Chem. Mater., **Just Accepted Manuscript** • DOI: 10.1021/acs.chemmater.0c01794 • Publication Date (Web): 06 Jul 2020

One-dimensional lead-free halide with near-unity greenish-yellow light emission

Sai Li,[†] Jun Xu,[†] Zhigang Li,[†] Zhichao Zeng,[†] Wei Li,[†] Minghuan Cui,[‡] ChaoChao Qin[‡] and Yaping Du[*,†]

[†]Tianjin Key Lab for Rare Earth Materials and Applications, Center for Rare Earth and Inorganic Functional Materials, School of Materials Science and Engineering & National Institute for Advanced Materials, Nankai University, Tianjin 300350, P.R. China.

[‡]Henan Key Laboratory of Infrared Materials & Spectrum Measures and Applications, Henan Normal University, Xinxiang 453007, P. R. China.

ABSTRACT: Low-dimensional metal halides (LDMHs), especially lead-based perovskites, have recently attracted extensive attention for their unique structures and optoelectronic properties. However, the toxicity of lead limits their practical applications. Herein, a lead-free 1D copper-based halide $[KC_2]_2[Cu_4I_6]$ (C = 12-crown-4 ether) was constructed, which exhibits greenish-yellow emission (545 nm) with a near-unity photoluminescence quantum yield (~97.8%). As far as we are aware, this is the highest value that has been achieved in lead-free greenish-yellow light-emitting LDMHs. Density functional theory calculations combined with comprehensive spectroscopic data revealed the characteristics of self-trapped excitons emission. Finally, we explored the application of $[KC_2]_2[Cu_4I_6]$ phosphor by fabricating the white light emitting diodes (WLEDs) device. The WLEDs fabricated using commercially available blue (450 nm) and ultraviolet LEDs (365nm) as the excitation source both present excellent luminescence properties with a high color rendering index and suitable corresponding color temperature. Our findings not only expand the library of high-efficient luminescent materials, but also highlight the potential of low-dimensional copper-based halide in optoelectronics.

INTRODUCTION

Lead halide perovskites have received great attention in recent years for their outstanding performance in a variety of optoelectronic applications owing to their excellent optical and electronic properties.[1-4] The unique structural modulability of the materials allows for a variety of connectivity between metal halides, from three-dimensional (3D) networks to two-dimensional (2D) layers, to one-dimensional (1D) chains, and finally to isolated zero-dimensional (0D) structures.[5-8] Among them, low dimensional metal halides exhibit unique photophysical properties because of strong quantum confinement effects. According to the mechanism proposed by Hemamala, the dimensionality of the crystal structure affects the self-trapped excitons (STEs) which are caused by soft lattice and the exciton−phonon interactions.[5-6] In the low-dimensional metal halides, metal polyhedra is separated by surrounding organic or inorganic ions, leading to strong exciton recombination and high efficiency self-trapped exciton emission.[9-13]

One of the noticeable problems that may restrict the application of halide perovskite materials is the toxicity of lead.[14] It is therefore necessary to develop lead-free metal halide materials comprising environment-friendly metals.[15-17] Compared with other metals, copper has attracted the attention of researchers because of its abundant reserves, low cost and non-toxicity.[18-20] Moreover, copper-based metal halides can readily form low-dimensional structures because of the small ionic radius.[21,22] Recently, several low-dimensional copper-based halides with high photoluminescence quantum yield have been reported.[9,10,18,19,22] 0D $Cs_3Cu_2I_5$ single crystal gives a broadband blue emission with a large Stokes shift and a photoluminescence quantum yield (PLQY) of 91.2%,[9] making it a promising candidate for the down-conversion light emitting diodes (LEDs). However, the peak wavelength of excitation spectrum is located at about 290 nm, which is in the range of deep ultraviolet (200−350 nm). The same problem exists in other reported inorganic low-dimensional halide structures of copper(I), adding to the difficulty for practical LEDs applications.[10,20,23,24] Here, we have

synthesized a copper-based organic-inorganic hybrid metal halide structure and found it possesses high-efficiency luminescent emission.[25] As revealed by density functional theory (DFT) calculations, in 1D $[KC_2]_2[Cu_4I_6]$, the 1D chains composed of copper halide tetrahedrons contribute to most electronic states, and the organic part only forms a 1D electronic structure with isolated $[Cu_4I_6]^{2-}$ in 2D direction. The degree of exciton delocalization greatly affects the radiative recombination rate.[26,27] Therefore, the $[KC_2]_2[Cu_4I_6]$ single crystal gives a high PLQY~97.8% and with a large Strokes shift of 145 nm at room temperature. Meantime, the peak wavelength of excitation spectrum of $[KC_2]_2[Cu_4I_6]$ covers 360–430 nm, which is well compatible with the LEDs ultraviolet chip and blue chip.

EXPERIMENTAL SECTION

Chemicals. CuI (99.998%) was purchased from Shanghai Macklin Biochemical Co., Ltd. KI was purchased from Tianjin Fengchuan Chemical Reagent Technologies Co., Ltd. 12-Crown-4 was purchased from the Alfa Aesar company. All of the chemicals were used without further purification.

Preparation of $[KC_2]_2[Cu_4I_6]$. Potassium iodide (2 g, 12 mmol), 12-crown-4 (0.88 g, 5 mmol) and copper(I) iodide (1 g, 5 mmol) were dissolved in acetone (50 mL). The solution was stored for a month at 252 K, allowing potassium iodide to crystallize. The suspension was filtered to remove the precipitates, and from the obtained yellow solution, single crystals of the title compound were obtained within one day by evaporation of the solvent at room temperature.

Characterizations. Powder X-ray diffraction (PXRD) data were collected on a Rigaku diffractometer using the Cu Ka radiation (λ = 1.5418 Å). Samples were scanned for every 0.02° increment over the Bragg angle range of 5-50°. X-ray photoelectron spectroscopy (XPS) measurement were done with a Thermo Scientific ESCALAB 250Xi spectrometer using a monochromatic Al Kα X-ray source (hν = 1486.6 eV) as the excitation source. The accurate binding energies (± 0.1 eV) were determined relative to the position of the C 1s peak at 284.8 eV. Thermogravimetric analysis (TGA) experiments were performed with a Mettler TGA/DSC3+ instrument at a heating rate of 10 K/min from 303 K to 1123 K under N_2 atmosphere. Steady-state absorption measurement was performed with a SHIMADZU UV-2600 UV–Vis–NIR spectrometer using $BaSO_4$ powder as the reflectance reference. Room-temperature PL emission and excitation spectra were recorded on an Edinburgh Instruments FLS1000 luminescence spectrometer. The PLQY measurements were performed on the same spectrometer using an integrating sphere. Temperature-dependent PL emission spectra were measured on an Edinburgh Instruments FLS 920 luminescence spectrometer, equipped with an OptistatDN variable liquid nitrogen cryostat (Oxford Instruments). Room temperature time-resolved PL emission data were collected at room temperature using an Edinburgh Instruments FLS1000 spectrometer. The dynamics of emission decay were monitored with the FLS1000's time-correlated single-photon counting capability (1024 channels; 200 μs window) with data collection for 10,000 counts. Excitation was provided by an Edinburgh EPL-360 picosecond pulsed diode laser. The lifetime was obtained by single-exponential fitting. Temperature-dependent time-resolved PL emission data were collected on an Edinburgh Instruments FLS 920 luminescence spectrometer, equipped with an OptistatDN variable liquid nitrogen cryostat (Oxford Instruments). Temperature control was achieved using an Omega CYC3200 autotuning temperature controller. Liquid nitrogen was used to cool the system. The power dependent PL measurements data was vertically collected and detected with a fiber spectrometer (USB-4000, Ocean Optics) using a

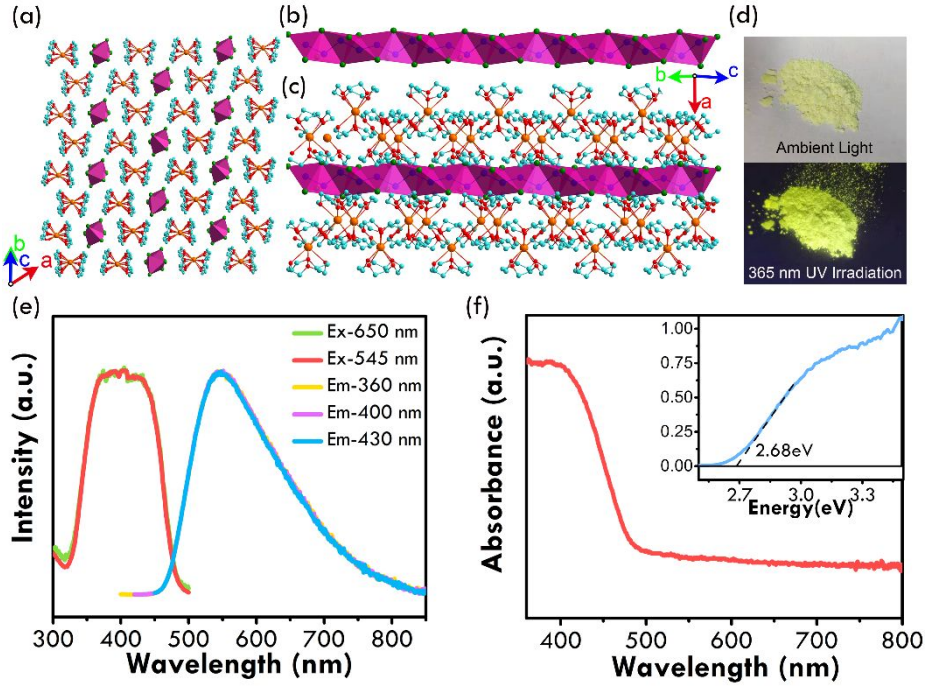

Figure 1. (a) Crystal structure of $[KC_2]_2[Cu_4I_6]$ (orange: potassium atoms; green: iodine atoms; blue: copper atoms; red: oxygen; aqua: carbon atoms; pink polyhedron: CuI_4 tetrahedra; hydrogen atoms were hidden for clarity). (b) Side view of an individual copper iodine chain. (c) Side view of an individual copper iodine chain with the organic cations. (d) Images of $[KC_2]_2[Cu_4I_6]$ under ambient light and UV irradiation (365 nm). (e) Excitation and emission spectra of $[KC_2]_2[Cu_4I_6]$ at different wavelengths. (f) Optical diffuse reflection spectra and corresponding Tauc plots (inset) of $[KC_2]_2[Cu_4I_6]$.

portion of the fundamental 800-nm laser pulses (Coherent, 800 nm, 1 kHz, 7 mJ pulse-1, 35 fs) directed vertically onto the quasi-2D RPP thin films via a neutral density filter (Daheng Optics, GCM-PS0720M) as the excitation source. The diameter of spot is about 5.1 mm.

Calculation details. All calculations for $[KC_2]_2[Cu_4I_6]$ were based on density functional theory (DFT) using the Vienna ab into simulation package (VASP) code.[28]The electron wave function was expanded through the plane wave basis set, and the projector augmented wave method (PAW) pseudopotentials were used to establish an effective interaction between valence electrons and atomic cores. Hence, few plane waves could be used in the calculation of the amount, but the accuracy was not affected. The generalized gradient approximation (GGA)-Perdew-Burke-Ernzerhof (PBE) functional was used to optimize structure through the relaxation of both the unit cell parameters and the atomic positions.[29] The PBE functional was also used in the calculation of the band structure and density of states (DOS). The self-consistent cycle cutoff condition in the calculation is that the residual forces on the atom were less than 0.001 eV/Å. The total energy converged to within 10^{-7} eV in the band structure and density of states calculations. The kinetic energy cutoff used in the calculation was 520 eV, and the mesh samplings in the Brillouin zone were 2*2*2. The Gaussian smearing method was used for self-consistent fields and band structure calculations, and the tetrahedron method with Blochl corrections was used for DOS calculations.

RESULTS AND DISCUSSION

The $[KC_2]_2[Cu_4I_6]$ single crystals were synthesized by solvent evaporation method. Typically, because of the d^{10} closed shell of Cu(I), Cu(I) halides tend to have a tetrahedral geometry.[30] Figure 1a-c show the crystal structure of $[KC_2]_2[Cu_4I_6]$ (unit cell: a = 67.4428, b = 69.0664, c = 64.1181 Å, α = 14.5859, β = 14.6371, and γ = 15.6526°), which belongs to the triclinic space group of P-1.[25] It consists of sandwich-type $[(12\text{-crown-}4)_2K]^+$ complex cations and polymeric $[Cu_4I_6]^{2-}$ anions. The latter is composed of CuI_4 tetrahedra, which share edges and faces to form infinite chains, as shown in Figure 1b. The crystal structure of $[(12\text{-crown-}4)_2K]^+$ complex cations and two adjacent inorganic CuI_4 units are shown in Figure S1. The 1D cooper halide chains are isolated from each other separated by organic ions. Figure S2 shows the comparison between$[KC_2]_2[Cu_4I_6]$ and other reported 1D light-emitting structures, including Ru_2CuBr_3 and $CsCu_2I_3$.[10,23] Different from the single chain of $CsCu_2I_3$ composed through $[CuI_4]^{3-}$ sharing corners and the double chain of Ru_2CuBr_3 composed through $[CuBr_4]^{3-}$ sharing edges, $[KC_2]_2[Cu_4I_6]$ has a unique zigzag-type chain, from which some different photophysical properties can be expected. From Figure S3 we can see the diffraction peaks of potassium iodide, which does not affect the measurement of photophysical properties. Other than these features, the powder X-ray diffraction (PXRD) pattern of the grinded powders of the single crystals has almost the same features as the simulated PXRD pattern. Moreover, we performed X-ray photoelectron spectroscopy (XPS) on the $[KC_2]_2[Cu_4I_6]$ sample to analyze the valance of copper (Figure S4). We noticed that the binding energies of 932.3 eV and 952.1 eV corresponding to Cu(I) $2p_{3/2}$ and Cu $2p_{1/2}$, respectively.[31] Besides, the binding energies of divalent Cu^{2+} are 942.4 eV and 962.3 eV, thus excluding the presence of divalent copper in the sample.[32]

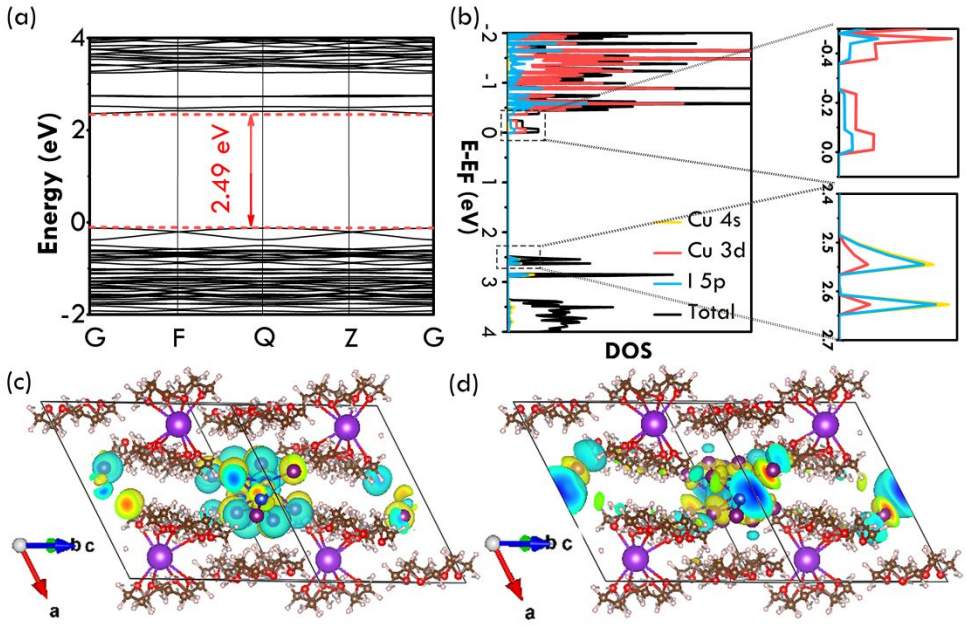

Figure 2. (a) Electronic band structure and (b) PDOS of calculated using the PBE functional. Note that the band gap is underestimated by the PBE calculations. (c, d) The isosurface plots of the wave function $|\Psi|^2$ of CBM and VBM.

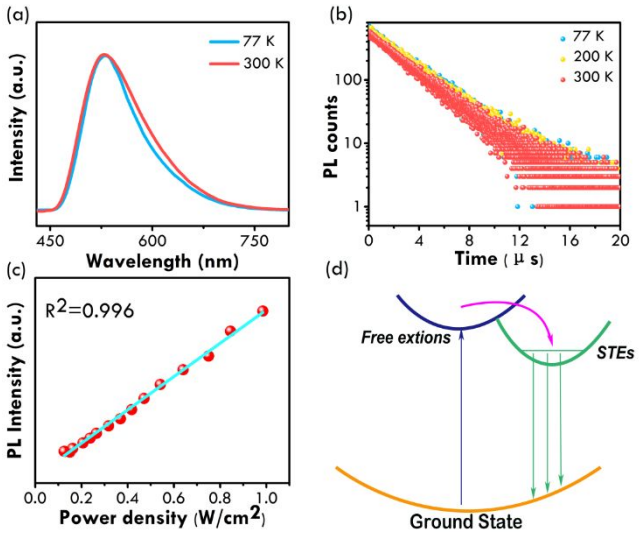

Figure 3. (a) Emission spectra and (b) emission decay curves of $[KC_2]_2[Cu_4I_6]$ at different temperatures. (c) Power-dependent PL (λ_{ex} = 365 nm) intensity of crystals of $[KC_2]_2[Cu_4I_6]$ (red circles) and the fitted data (turquoise line). (d) Schematic diagram of the photophysical processes.

As shown in Figure 1d, the sample emits bright greenish-yellow light when exposed to ultraviolet (UV) light (365 nm). The photophysical properties are further characterized. The emission spectrum of the sample has a peak at 545 nm with a full width at half maxima of 145 nm at room temperature, and the emission spectra obtained under different excitation wavelengths (360 nm, 400 nm, 430 nm) are almost identical (Figure 1e). Figure S5 shows the excitation and emission spectra on the PLQY determination. The quantum yield of greenish-yellow emission is calculated to near-unity (97.8%). To the best of our knowledge, this is the highest PLQY obtained in lead-free based greenish-yellow light-emitting halides. Compared with other greenish-yellow halide perovskites and relevant materials, $[KC_2]_2[Cu_4I_6]$ has the prominent advantages in safety and efficiency (Table S1). Also, we noticed that $[KC_2]_2[Cu_4I_6]$ has a very large Stokes shift of about 145 nm. Typically, PL spectra with such large Stokes shifts are attributed to STEs as a result of strong exciton–phonon coupling.[13,33,34] The peak of the excitation wavelength has a plateau covering 360–430 nm, which is consistent with the absorption spectrum.

According to the absorption spectrum, we calculated that the band gap is 2.68 eV (Figure 1f). The luminescence decay at room temperature shows a long lifetime of 2.6 microseconds by mono-exponential fitting, similar to other low-dimensional metal halides, and consistent with the characteristics of exciton self-trapped emission.[35] Broad emission with a long lifetime is a characteristic of Cu(I)-complexed phosphorescent emissions involving Jahn–Teller distortion.[30] Meantime, the tetrahedral structure formed by fourfold coordinated Cu atoms and halides ions also favors the Jahn–Teller distortion to produce strong STEs emission.[9,24] We noticed that the emission peak had a relatively long tail, which can also be seen in other cooper-based halides.[10,22,36] And the fluorescence lifetimes monitored at different emission wavelengths are completely identical, indicating that the emission comes from the same launch center (Figure S6).

In order to further understand the electron properties of the sample, we use PBE functional to calculate the band structure and density of states from DFT. As shown in Figure 2a, $[KC_2]_2[Cu_4I_6]$ has a direct band gap, with the CBM and VBM both at the point G. The gap is calculated to be 2.49 eV, which is slightly smaller than the experimental value (2.68 eV). This can be attributed to the errors of PBE calculation.[9] The valence band maximum (VBM) is mostly made up by Cu-3d and I-5p states, whereas the conduction band minimum (CBM) is mainly made up by Cu-4s and I-5p states (Figure 2b). The organic cation part does not contribute to CBM and VBM, which can also be proved by the isosurface plots of the wave function $|\Psi|^2$ of CBM and VBM (Figure 2c, d). Therefore, the structure can be seen as two parts: 1D copper halide chains, and organic cations as the isolator.

To further investigate the mechanism of emission, low-temperature emission spectrum and emission delay curve were investigated. At 77 K, the emission spectrum becomes narrower because of the decrease of the dynamic thermal filling vibration at low temperatures,[11] whereas the position of the emission peak is basically invariant (Figure 3a). The corresponding PL decay curve of $[KC_2]_2[Cu_4I_6]$ (Figure 3b) gives a long average lifetime of 2.68 μs by single exponential fitting. The PL lifetime is almost invariant with the temperature decreased, which is characteristic of phosphorescence.[37] That further indicates the broadband emission is not due to multiple radiation mechanisms. The emission intensity of permanent defects generally has a sublinear dependence on the excitation power. When all defects are excited, they eventually reach saturation.[5] Therefore, the existence of permanent defects were excluded as the origin of the photoemission by the linear dependence of excitation power and fluorescence intensity (Figure 3c). Meanwhile, the shape of the peak remains unchanged (Figure S7). Based on the above results, we proposed a configuration coordinate diagram which is common in low-dimensional metal halides to describe the photophysical processes in 1D $[KC_2]_2[Cu_4I_6]$. Upon photoexcitation, the electron of $[Cu_4I_6]$ are excited to the excited state from ground state. Free excitons are produced first, they will be quickly self-trapped to form STEs due to the structural distortion of the polyhedron, then STEs transit from singlet to triplet states, which back to ground state resulting in relatively strong Stokes-shifted broadband luminescence in $[KC_2]_2[Cu_4I_6]$.[22]

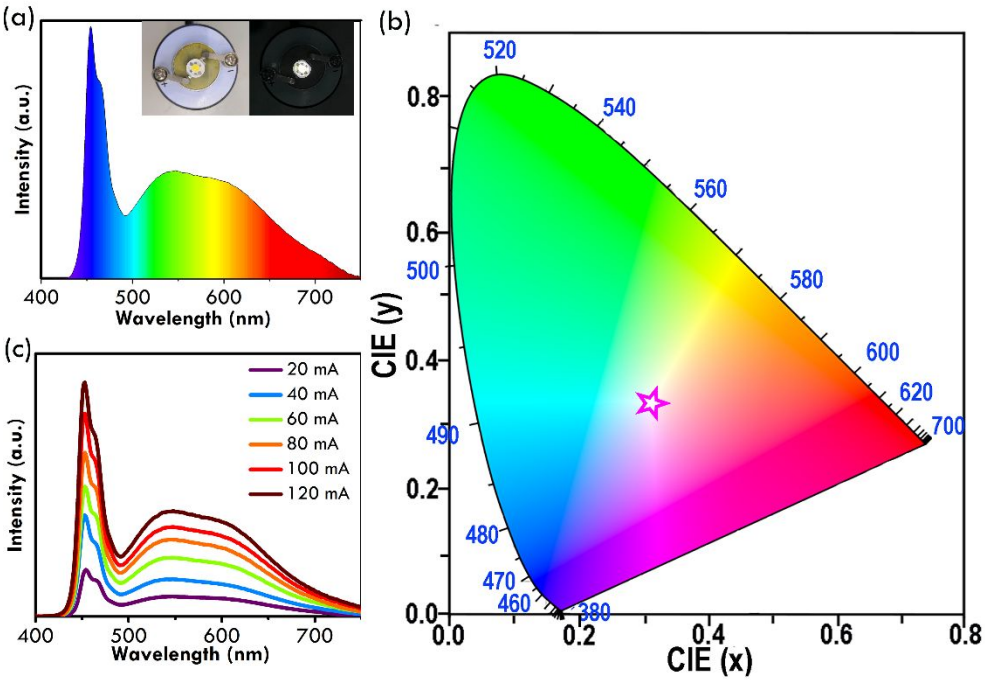

Figure 4. (a) Luminescence spectrum from $[KC_2]_2[Cu_4I_6]$-based white-light-emitting diodes (LEDs) excited with a 450 nm blue chip and (inset) photo of an operating LED. (b) CIE coordinates corresponding to white-LED device (pink star). (c) The emission spectra of white-LED device at different driving currents.

Figure S8 shows the structural and photoluminescence stability of $[KC_2]_2[Cu_4I_6]$. We compared the PXRD patterns of sample stored for a week with the pristine patterns (Figure S8a). No additional peaks were observed, indicating the good structural stability of the obtained compounds. And there was no significant change in fluorescence intensity or lifetime after stored for a week or irradiation for 3 hours. Combined with stable QY (›90%), $[KC_2]_2[Cu_4I_6]$ shows great photostability and air stability.

The near-unity PLQY in the solid state makes this lead-free material highly promising light emitters for a variety of applications. Meantime, the strongly shifted broadband emission with minimal self-absorption and good thermal stability (Figure S9) is of particular interest for applications in down conversion white light emitting diodes (WLEDs) and luminescent solar concentrators. To demonstrate the use of this material as a phosphor, we fabricated the down-conversion WLEDs using a commercially available blue LEDs (450 nm) as the excitation (Figure 4a). Commercial red-emitting phosphors (Ca, Sr)$AlSiN_3$:Eu^{2+} and the sample were mixed to form a film as the emission source. The WLEDs was obtained with the high color rendering index (CRI) of 86.5, CCT of 5834 K, and a CIE color coordinate of (0.32,0.33) (Figure 4b). Excellent color stability was observed in this white LEDs at different operating currents (20–120 mA), as shown in Figure 4c. After running at 10mA for 10 hours, the intensity of the device can be maintained at 80%, shows good stability (Figure S10). To demonstrate good compatibility with LEDs chips, we also assembled a down-conversion WLED with a UV chip (365 nm). The WLEDs presented good luminescence properties with a high CRI of 86, CCT of 6411 K, and a CIE color coordinate of (0.31,0.3) (Figure S11).

CONCLUSIONS

We report a new high-efficiency 1D lead-free luminescent metal halide $[KC_2]_2[Cu_4I_6]$, which consists of sandwich-type $[(12\text{-crown-}4)_2K]^+$ complex cations and polymeric $[Cu_4I_6]^{2-}$ 1D chains. This compound provides an interesting example of replacing lead with the environment-friendly and inexpensive cooper to achieve efficient visible light emission. DFT calculation revealed the direct band gap semiconducting behavior of $[KC_2]_2[Cu_4I_6]$, and the 1D electronic structure. PL measurements indicated that upon 365 nm excitation, $[KC_2]_2[Cu_4I_6]$ exhibits strong broadband greenish-yellow emission centered at 545 nm with a tail at lower energy covering the red region. More importantly, the compound exhibits a near-unity PLQY of ~97.8%, which is the highest value that has been achieved in lead-free greenish-yellow light-emitting LDMHs. Besides, $[KC_2]_2[Cu_4I_6]$ shows excellent stability. Finally, the WLEDs fabricated by combining the greenish-yellow-emitting $[KC_2]_2[Cu_4I_6]$ with commercial red phosphors exhibits a high CRI of 86.5 and CCT of 5834 K, demonstrating the potentials of $[KC_2]_2[Cu_4I_6]$ for application in solid-state lighting. Our findings advance the research in organic inorganic hybrid low-dimensional metal halide and highlight the potential of low-dimensional copper-based halide for optoelectronic applications.

ASSOCIATED CONTENT

Supporting Information. Comparison of PLQY values of the halide with other relevant materials; Crystal structure of $[(12\text{-crown-}4)_2K]^+$ ions and two adjacent inorganic CuI_4 units; Chain structure of different 1D copper(I)-based halides; XRD, PLQY, TGA, PL lifetime and XPS of $[KC_2]_2[Cu_4I_6]$, stability of $[KC_2]_2[Cu_4I_6]$ and WLEDs, and WLED with 365 nm chip.

AUTHOR INFORMATION

Corresponding Author

* Email: ypdu@nankai.edu.cn

Funding Sources

We acknowledge the financial support from the National Natural Science Foundation of China (21522106 and 21971117), 111 Project (B18030) from China, the National Key R&D Program of China (No. 2017YFA0208000), the Open Funds (RERU2019001) of the State Key Laboratory of Rare Earth Resource Utilization and the Functional Research Funds for the Central Universities, Nankai University (63186005). We also thank Prof. Xueyuan Chen of Fujian Institute of Research on the Structure of Matter for kind help and discussions.

Notes

The authors declare that they have no conflict of interest.

REFERENCES

(1) Protesescu, L.; Yakunin, S.; Bodnarchuk, M. I.; Krieg, F.; Caputo, R.; Hendon, C. H.; Yang, R. X.; Walsh, A.; Kovalenko, M. V. Nanocrystals of Cesium Lead Halide Perovskites ($CsPbX_3$, X = Cl, Br, and I): Novel Optoelectronic Materials Showing Bright Emission with Wide Color Gamut. *Nano Lett.* **2015**, *15*, 3692-3696.

(2) Zhang, F.; Zhong, H.; Chen, C.; Wu, X. G.; Hu, X.; Huang, H.; Han, J.; Zou, B.; Dong, Y. Brightly Luminescent and Color-Tunable Colloidal $CH_3NH_3PbX_3$ (X = Br, I, Cl) Quantum Dots: Potential Alternatives for Display Technology. *ACS Nano* **2015**, *9*, 4533-4542.

(3) Cui, B. B.; Han, Y.; Huang, B.; Zhao, Y.; Wu, X.; Liu, L.; Cao, G.; Du, Q.; Liu, N.; Zou, W.; Sun, M.; Wang, L.; Liu, X.; Wang, J.; Zhou, H.; Chen, Q. Locally Collective Hydrogen Bonding Isolates Lead Octahedra for White Emission Improvement. *Nat. Commun.* **2019**, *10*, 5190.

(4) Zhou, C.; Lin, H.; He, Q.; Xu, L.; Worku, M.; Chaaban, M.; Lee, S.; Shi, X.; Du, M. H.; Ma, B. Low Dimensional Metal Halide Perovskites and Hybrids. *Mat. Sci. Eng. R,* **2019**, *137*, 38-65.

(5) Dohner, E. R.; Hoke, E. T.; Karunadasa, H. I. Self-Assembly of Broadband White-Light Emitters. *J. Am. Chem. Soc.* **2014**, *136*, 1718-1721.

(6) Dohner, E. R.; Jaffe, A.; Bradshaw, L. R.; Karunadasa, H. I. Intrinsic White-Light Emission from Layered Hybrid Perovskites. *J. Am. Chem. Soc.* **2014**, *136*, 13154-13157.

(7) Dutta, A.; Behera, R. K.; Pal, P.; Baitalik, S.; Pradhan, N. Near-Unity Photoluminescence Quantum Efficiency for All $CsPbX_3$ (X = Cl, Br, and I) Perovskite Nanocrystals: A Generic Synthesis Approach. *Angew. Chem. Int. Ed.* **2019**, *58*, 5552-5556.

(8) Worku, M.; Tian, Y.; Zhou, C.; Lee, S.; Meisner, Q.; Zhou, Y.; Ma, B. Sunlike White-Light-Emitting Diodes Based on Zero-Dimensional Organic Metal Halide Hybrids. *ACS Appl. Mater. Interfaces* **2018**, *10*, 30051-30057.

(9) Jun, T.; Sim, K.; Iimura, S.; Sasase, M.; Kamioka, H.; Kim, J.; Hosono, H. Lead-Free Highly Efficient Blue-Emitting $Cs_3Cu_2I_5$ with 0D Electronic Structure. *Adv. Mater.* **2018**, *30*, 1804547.

(10) Yang, B.; Yin, L.; Niu, G.; Yuan, J. H.; Xue, K. H.; Tan, Z.; Miao, X. S.; Niu, M.; Du, X.; Song, H.; Lifshitz, E.; Tang, J. Lead-Free Halide Rb_2CuBr_3 as Sensitive X-Ray Scintillator. *Adv. Mater.* **2019**, *31*, 1904711.

(11) Zhou, C.; Lin, H.; Worku, M.; Neu, J.; Zhou, Y.; Tian, Y.; Lee, S.; Djurovich, P.; Siegrist, T.; Ma, B. Blue Emitting Single Crystalline Assembly of Metal Halide Clusters. *J. Am. Chem. Soc.* **2018**, *140*, 13181-13184.

(12) Zhou, J.; Li, M.; Ning, L.; Zhang, R.; Molokeev, M. S.; Zhao, J.; Yang, S.; Han, K.; Xia, Z. Broad-Band Emission in a Zero-Dimensional Hybrid Organic $[PbBr_6]$ Trimer with Intrinsic Vacancies. *J. Phys. Chem. Lett.* **2019**, *10*, 1337-1341.

(13) Zhou, L.; Liao, J. F.; Huang, Z. G.; Wei, J. H.; Wang, X. D.; Chen, H. Y.; Kuang, D. B.; Su, C. Y. Highly Red Emissive Lead-Free Indium-Based Perovskite Single Crystal for Sensitive Water Detection. *Angew. Chem. Int. Ed.* **2019**, 58, 5277-5281.

(14) Xiao, Z.; Meng, W.; Wang, J.; Mitzi, D. B.; Yan, Y. Searching for Promising New Perovskite-Based Photovoltaic Absorbers: the Importance of Electronic Dimensionality. *Mater. Horiz.* **2017**, *4*, 206-216.

(15) Roccanova, R.; Houck, M.; Yangui, A.; Han, D.; Shi, H.; Wu, Y.; Glatzhofer, D. T.; Powell, D. R.; Chen, S.; Fourati, H.; Lusson, A.; Boukheddaden, K.; Du, M. H.; Saparov, B. Broadband Emission in Hybrid Organic−Inorganic Halides of Group 12 Metals. *ACS Omega* **2018**, *3*, 18791-18802.

(16) Tan, Z.; Li, J.; Zhang, C.; Li, Z.; Hu, Q.; Xiao, Z.; Kamiya, T.; Hosono, H.; Niu, G.; Lifshitz, E.; Cheng, Y.; Tang, J. Highly Efficient Blue-Emitting Bi-Doped Cs_2SnCl_6 Perovskite Variant: Photoluminescence Induced by Impurity Doping. *Adv. Funct. Mater.* **2018**, *28*, 1801131.

(17) Zhang, R.; Mao, X.; Yang, Y.; Yang, S.; Zhao, W.; Wumaier, T.; Wei, D.; Deng, W.; Han, K. Air-Stable, Lead-Free Zero-Dimensional Mixed Bismuth-Antimony Perovskite Single Crystals with Ultra-broadband Emission. *Angew. Chem. Int. Ed.* **2019**, *58*, 2725-2729.

(18) Lin, H.; Zhou, C.; Neu, J.; Zhou, Y.; Han, D.; Chen, S.; Worku, M.; Chaaban, M.; Lee, S.; Berkwits, E.; Siegrist, T.; Du, M. H.; Ma, B. Bulk Assembly of Corrugated 1D Metal Halides with Broadband Yellow Emission. *Adv. Optical Mater.* **2019**, *7*, 1801474.

(19) Luo, Z.; Li, Q.; Zhang, L.; Wu, X.; Tan, L.; Zou, C.; Liu, Y.; Quan, Z. 0D $Cs_3Cu_2X_5$ (X = I, Br, and Cl) Nanocrystals: Colloidal Syntheses and Optical Properties. *Small* **2019**, 1905226.

(20) Roccanova, R.; Yangui, A.; Seo, G.; Creason, T. D.; Wu, Y.; Kim, D. Y.; Du, M. H., Saparov, B. Bright Luminescence from Nontoxic $CsCu_2X_3$ (X = Cl, Br, I). *ACS Mater. Lett.* **2019**, *1*, 459-465.

(21) Shi, Z.; Guo, J.; Chen, Y.; Li, Q.; Pan, Y.; Zhang, H.; Xia, Y.; Huang, W. Lead-Free Organic-Inorganic Hybrid Perovskites for Photovoltaic Applications: Recent Advances and Perspectives. *Adv. Mater.* **2017**, *29*, 1605005.

(22) Cheng, P.; Sun, L.; Feng, L.; Yang, S.; Yang, Y.; Zheng, D.; Zhao, Y.; Sang, Y.; Zhang, R.; Wei, D.; Deng, W.; Han, K. Colloidal Synthesis and Optical Properties of All-Inorganic Low-Dimensional Cesium Copper Halide Nanocrystals. *Angew. Chem. Int. Ed.* **2019**, *58*, 16087-16091.

(23) Lin, R.; Guo, Q.; Zhu, Q.; Zhu, Y.; Zheng, W.; Huang, F. All-Inorganic $CsCu_2I_3$ Single Crystal with High-PLQY (≈15.7%) Intrinsic White-Light Emission via Strongly Localized 1D Excitonic Recombination. *Adv. Mater.* **2019**, *31*, 1905079.

(24) Roccanova, R.; Yangui, A.; Nhalil, H.; Shi, H.; Du, M. H.; Saparov, B. Near-Unity Photoluminescence Quantum Yield in Blue-Emitting $Cs_3Cu_2Br_{5-x}I_x$ ($0 \le x \le 5$). *ACS Appl. Electron. Mater.* **2019**, *1*, 269-274.

(25) Paulsson, H.; Fischer, A.; Kloo, L. Bis[bis(12-crown-4)-potassium] hexa-iodo-tetra-cuprate(I). *Acta Crystallogr. E* **2004**,

60, m548-m550.

(26) Mao, L.; Guo, P.; Kepenekian, M.; Hadar, I.; Katan, C.; Even, J.; Schaller, R. D.; Stoumpos, C. C.; Kanatzidis, M. G. Structural Diversity in White-Light-Emitting Hybrid Lead Bromide Perovskites. *J. Am. Chem. Soc.* **2018**, *140*, 13078-13088.

(27) Wu, G.; Zhou, C.; Ming, W.; Han, D.; Chen, S.; Yang, D.; Besara, T.; Neu, J.; Siegrist, T.; Du, M. H.; Ma, B.; Dong, A. A One-Dimensional Organic Lead Chloride Hybrid with Excitation-Dependent Broadband Emissions. *ACS Energy Lett.* **2018**, *3*, 1443-1449.

(28) Kresse, G.; Furthmüller, J. Efficiency of Ab-initio Total Energy Calculations for Metals and Semiconductors Using a Plane-Wave Basis Set. *Comput. Mater. Sci.* **1996**, *6*, 15–50.

(29) Perdew, J. P.; Burke, K.; Ernzerhof, M. Generalized Gradient Approximation Made Simple. *Phys. Rev. Lett.* **1997**, *78*, 1396-1396.

(30) Xiao, Z.; Du, K. Z.; Meng, W.; Mitzi, D. B.; Yan, Y. Chemical Origin of the Stability Difference between Copper(I)- and Silver(I)-Based Halide Double Perovskites. *Angew. Chem. Int. Ed.* **2017**, *129*, 12107-12111.

(31) Bi, C.; Wang, S.; Li, Q.; Kershaw, S. V.; Tian, J.; Rogach, A. L. Thermally Stable Copper (II)-Doped Cesium Lead Halide Perovskite Quantum Dots with Strong Blue Emission. *J. Phys. Chem. Lett.* **2019**, 10, 943-952.

(32) Liu, L.; Zhong, H.; Bai, Z.; Zhang, T.; Fu, W.; Shi, L.; Xie, H.; Deng, L.; Zou, B. Controllable Transformation from Rhombohedral $Cu_{1.8}S$ Nanocrystals to Hexagonal CuS Clusters: Phase- and Composition Dependent Plasmonic Properties. *Chem. Mater.* **2013**, *25*, 4828-4834.

(33) Zhou, C.; Lin, H.; Lee, S.; Chaaban, M.; Ma, B. Organic-Inorganic Metal Halide Hybids Beyond Perovskites. *Mater. Res. Lett.* **2018**, *6*, 552-569.

(34) Qin, Y.; Lv, Z.; Chen, S.; Li, W.; Wu, X.; Ye, L.; Li, N.; Lu, P. Tuning Pressure-Induced Phase Transitions, Amorphization and Excitonic Emissions of 2D Hybrid Perovskites via Varying Organic Amine Cations. *J. Phys. Chem. C* **2019**, *123*, 22491-22498.

(35) Kim, Y. E.; Kim, J.; Park, J. W.; Park, K.; Lee, Y. σ-Complexation as a Strategy for Designing Copper-based Light Emitters. *Chem. Commun.* **2017**, *53*, 2858-2861.

(36) Lin, J.; Chen, H.; Kang, J.; Quan, L. N.; Lin, Z.; Kong, Q.; Lai, M.; Yu, S.; Wang, L.; Wang, L. W.; Toney, M. F.; Yang, P. Copper(I)-Based Highly Emissive All-Inorganic Rare-Earth Halide Clusters. *Matter* **2019**, *1*, 180-191.

(37) Liu, W.; Fang, Y.; Li, J. Copper Iodide Based Hybrid Phosphors for Energy-Efficient General Lighting Technologies. *Adv. Funct. Mater.* **2018**, *28*, 1705593.